JOURNAL OF CATALYSIS 152, 384–395 (1995)

Surface Characterization of Modified Aluminas

III. Surface Features of PO_4-Doped Al_2O_3

C. Morterra,* G. Magnacca,* and P. P. De Maestri†

Department of Inorganic, Physical, and Materials Chemistry, University of Turin, via P. Giuria 7, I-10125 Turin, Italy; and †Centro Ricerche Fiat, Strada Torino 50, I-10043 Orbassano, Turin, Italy

Received July 5, 1994; revised November 29, 1994

Pure and PO_4-doped aluminas (≈3% P_2O_5), pretreated at three different temperatures (773, 1273, and 1473 K), have been compared by XRD, TEM, and FTIR spectroscopy. The addition of phosphates does not modify the phase transition of low-temperature spinel aluminas (γ-Al_2O_3) to high-temperature spinel aluminas (δ, θ-Al_2O_3), and delays somewhat the phase transition from spinel alumina to the corundum phase (α-Al_2O_3). Phosphates have a positive effect on surface area and porosity only for the corundum phase obtained at $T \geq 1450$ K, in which the particles morphology is modified with respect to pure α-Al_2O_3. The effect of PO_4-doping is appreciable on surface basicity and acidity. The weak basicity of alumina is gradually eliminated, with increasing firing temperature. The presence of phosphates increases the strong surface acidity of aluminas: phosphates tend to collect preferably on the flat patches of regular crystal planes, and so doing decrease the amount and increase the strength of the Lewis acid sites (coordinatively unsaturated (cus) Al^{IV} ions) present on the regular crystal planes. Meanwhile, the presence of phosphates produces an appreciable increase of the number of strong cus Al^{IV} Lewis acid sites present in crystallographically and/or coordinatively defective configurations. When the bulk transition to α-Al_2O_3 has occurred in systems treated at $T \geq 1400$ K, the samples retain surface properties reminiscent of those of the transition alumina phases. The diverse opinion of investigators that phosphates act toward alumina as phase stabilizing needs some corrections and additions: the positive role of phosphates on the alumina support implies the stabilization of higher amounts of the strong Lewis acid sites that are most likely to be important in catalytic applications. © 1995 Academic Press, Inc.

INTRODUCTION

Transition-phase (spinel) aluminas (1) are seldom used as catalysts as such but far more often as metal catalyst support. This is, for instance, the case of the widespread application of alumina in the porous washcoat layer of three-way automotive catalytic converters. In various catalytic applications, the active Al_2O_3 layer may be subjected to severe chemical and/or physical damage, among which trace chemical contamination and thermal stress are most important. As for the latter effect, it can produce loss of surface area, pore blockage, and undesired crystal phase transition(s). For this reason, catalytic Al_2O_3 is often doped with small amounts of other elements, that are empirically observed to improve the overall performance of the substrate and are supposed to act as crystal phase and/or surface area stabilizers.

The use of phosphates as promoting additives for catalytic aluminas has been reported in some instances, and their effect has been suggested to be twofold. Phosphates have been claimed to play the role of support stabilizers (2), and to modify in a potentially convenient way some of the acid-base surface properties of the active carrier (2–8).

The support stabilizing effect, that has not been investigated yet in much detail on a microscopic scale, seems to delay the most undesired phase transition γ-$Al_2O_3 \rightarrow \alpha$-$Al_2O_3$ (2) and the relevant decline of surface area, and also to affect the transition amorphous $Al_2O_3 \rightarrow \gamma$-$Al_2O_3$ (9). This behaviour may be thought of as being one particular aspect of a more general phenomenon, by which the presence of anionic groups at the surface of oxidic systems tends to broaden the temperature range of existence of some metastable crystal phases (typical is the case of tetragonal ZrO_2, that remains stable at temperatures as high as ≈1000 K when carrying surface sulfates (10, 11).

As for the surface chemical modifications brought about by phosphates, [PO_4] units have been reported to accumulate as such at the surface of alumina (adsorbing through a specific acid-base interaction with alumina surface hydroxyls (8) for concentrations up to the completion of an appreciable fraction of a monolayer, and then to accumulate preferably in the form of polyphosphates (8, 12). Surface basicity of alumina was found to be somewhat diminished by surface phosphates (4), whereas surface acidity of alumina was reported to be increased first, though to a moderate extent (4, 6, 7), and then to decline (2, 8), depending on the amount of phosphates added.

0021-9517/95 $6.00

The present paper deals with the effect of the addition of a small amount of P_2O_5 (≈3% wt) to a well-defined transition-phase alumina (13), i.e., of an amount of P of the order normally employed as a surface area and/or phase stabilizer. The effect of phosphates will be considered from the point of view of the structural, morphological, and surface chemical features and will be examined in a wide range of sample calcination temperatures (773–1473 K). In fact this work is mainly aimed at the understanding of the role played by phosphate additives, and/or by possible P-containing contaminants, on a washcoat alumina layer that works routinely at 800–1100 K, but can exceptionally experience temperatures as high as ≈1500 K.

EXPERIMENTAL

Materials. Pure alumina samples and phosphate-doped alumina samples, defined in a recent patent as "Stabilized Active Al_2O_3 Support" (13), were prepared starting from pure commercial boehmite (Disperal Alumina, Condea Chemie), following a procedure described in detail in previous notes (14, 15). In particular, phosphates were added to the acidic suspension (pH = 3) of boehmite in the form of phosphoric acid, in an amount that was calculated in order to yield a nominal concentration of 3 wt% P_2O_5 in the γ-Al_2O_3 phase resulting from the thermal decomposition of the Al hydroxide precursor.

Pure and doped alumina specimens were fired in the air for 3 h at three temperatures (773, 1273, and 1473 K), rehydrated by exposure to the atmosphere, and stored in a closed glass vessel. Samples were prepared for IR measurements in the form of self-supporting pellets (15–25 mg cm^{-2}) and, occasionally, in the form of thin layer films (5–10 mg cm^{-2}) deposited from aqueous suspension over a pure Si platelet. Thermal treatments were carried out at the chosen temperature in the IR cell, first *in vacuo* for 2 h (residual pressure $\leq 10^{-5}$ Torr; 1 Torr = 133.3 N m^{-2}), and for the last 30 min in O_2 (≈100 Torr).

Samples are designated in the text and figure captions by the symbols A (reference pure alumina) and AP (phosphate-doped alumina), followed by a subscript numeral T_1 (K), representing the oven firing temperature of the material, and a second numeral T_2 (K), representing the temperature of vacuum thermal activation/oxidation undergone by the sample prior to adsorption and IR investigation. Sometimes the symbol AP_{T_1} is followed by the letter a, meaning that the sample was aged in a closed vessel at ambient temperature for several months.

Methods. BET surface areas were determined with N_2 at 78 K with an automatic apparatus (Sorptomatic 1900, C. Erba).

Crystal phases were determined with an X-ray diffractometer (Philips PW 1050) using Cu$K\alpha$ radiation.

Electron micrographs were obtained with an electron microscope Jeol JEM 2000 EX (200 kV acceleration), equipped with a top-entry stage; the alumina samples were dispersed in *n*-heptane and then deposited on Cu grids coated with a "holey" carbon film.

IR spectra were run at resolution 2 cm^{-1} on a Bruker 113v FTIR spectrometer equipped with MCT detector; from all spectra of adsorbed species, the contribution of the gaseous phase was computer subtracted interactively.

RESULTS AND DISCUSSION

Structural and Morphological Data

Table 1 summarizes some XRD, BET, and (nominal) phosphate loading data relative to A_{T_1} and AP_{T_1} preparations. The following can be noted.

(i) The presence of phosphate species does not modify to an appreciable extent the crystal phase of alumina samples treated at T_1 as high as ≈1300 K. In particular, the appearance and interconversion of the spinel alumina species (γ, δ, θ) is found to occur at the usual temperatures [1, 16]. Only the relative intensity of the XRD peaks is smaller for AP systems than for A systems, and the peaks breadth is definitely larger, suggesting for the P-doped materials a more disordered structure, i.e., smaller particles and/or a shorter range crystalline order.

(ii) The surface area of AP systems treated at T_1 as high as ≈1300 K is appreciably lower (≈20%) than that of the corresponding undoped A systems, indicating that the P-doped materials cannot have appreciably smaller particles (this would cause higher surface area), and that there is no surface area stabilization effect from phosphates in the case of the transition phase (spinel) aluminas.

(iii) The behavior of the AP_{1473} system is quite peculiar. The powdery AP_{1473} sample examined immediately after the preparation process indicates that the phase transi-

TABLE 1

Crystal Phase, Surface Area and Nominal P Content of Pure and PO_4-Doped Aluminas

Sample	Crystal phase	Surface area (m^2 g^{-1})	Nominal P content (PO_4 groups per nm^2)
A_{773}	γ	186	/
AP_{773}	γ	148	1.7
A_{1273}	δ(M); γ(m)	120	/
AP_{1273}	δ	99	2.5
A_{1473}	α	4.5	/
AP_{1473}	δ, θ(M); α(m)	53	4.7
$AP_{1473}a$*	α	≈20	≈12

Note. (M): major component; (m); minor component.
*a stands for aged material (several months at ambient temperature).

tion from the spinel phases to the corundum phase has occurred only to a very minor extent, while the surface area has declined by some 50%. But the same material, examined after long aging at ambient temperature (approximately one year, in the case examined here; this material is hereafter referred to as $AP_{1473}a$), indicates that the phase transition to the α-Al_2O_3 phase has occurred thoroughly. In fact the XRD pattern is now virtually indistinguishable from that of the A_{1473} system (in particular, no evidence is left for the XRD lines typical of transition phase aluminas), while the surface area has declined by a further $\approx$50%, still remaining appreciably higher than that of the corresponding A_{1473} system.

It is thus deduced that, when in a phosphate-doped alumina treated at high temperatures there is the formation of traces of the corundum phase, the latter acts as crystalline germs for a slow complete transformation of the whole transition phase system into the corundum phase. This effect can be expected to be appreciably faster in other conditions, for instance, in the more drastic temperature and moisture conditions experienced by a working catalyst, so that the claimed phase stabilizing properties of phosphate additives towards high temperature aluminas ought to be considered with caution.

Figure 1 reports some TEM micrographs of the AP_{T_1} specimens. Note that the images of the transition phase samples (1a and 1b) are quite pale, due to the high transparency to the electron beam of most Al_2O_3 microcrystalline systems (17). No specific sections are devoted in the figure to the images of the corresponding A_{T_1} systems, as they have been recently shown and described elsewhere (15, 17).

It can be noted that:

(i) The AP_{773} preparation (Fig. 1a) is made up of large aggregates of small crystallites ($\approx$5 nm side), stuck together in a highly disordered fashion: see, in particular, the top left-hand images in Fig. 1a, in which the faint interference fringe patterns cross with one another in a very disordered way. The overall aspect of the AP_{773} system suggests a low degree of crystallinity. In fact, very seldom do the ultimate crystallites exhibit the sharp edges and neat contours, typical of most γ-Al_2O_3 preparations (17) (see, for comparison, the inset to Fig. 1a, showing a detail of the A_{773} reference system). Most of the crystallites present irregular shape, roundish contours, and very small patches of regular (low index) crystal planes, as demonstrated by the very short range patterns of interference fringes. These morphological data suggest that the P-doped γ-Al_2O_3 system should possess a large proportion of crystallographically defective terminations, which should correspond to highly active surface sites.

(ii) The AP_{1273} preparation (Fig. 1b) is still made up of aggregat of crystallites, whose average size is now $\approx$7–8 nm. The crystallites are now characterized by definitely sharper contours than in the case of AP_{773} and by still highly stepped terminations (see, for instance, the detail in the inset to Fig. 1b). In this stage of the thermal sintering process, corresponding to the dominant presence of the δ-θ spinel phases, the morphological differences between pure and P-doped alumina specimens has become minimal (17).

(iii) The fresh AP_{1473} preparation presents only minor differences, if any, with respect to the AP_{1273} preparation, and for this reason it is not shown in the figure. The ultimate crystallites now possess further sharpened edges and further increased average size ($\approx$10–12 nm), but only occasionally can large and shapeless (pebble-like) particles, typical of α-Al_2O_3, be singled out.

The morphology of the aged $AP_{1473}a$ preparation, shown in Fig. 1c, is quite different from that of the other AP systems. This preparation has become difficult to examine in the transmission mode, due to the high opacity to the electron beam, and this indicates a much increased average size of the crystal aggregates. Wherever the contours of the large and thick particles can be examined at high resolution, one can notice that the termination of the aggregates (and thus the whole aggregates) is still reminiscent of the previous shape: the bulky particles are still made up of the original irregular crystallites, that are now somewhat more orderly and more intimately stuck together. This prevailing morphology explains, on one side, the decreased surface area of the material, and suggests, on the other side, that the $AP_{1473}a$ preparation should still possess abundant amounts of crystallographically defective terminations. The residual presence of surface active configurations should be detected with gas-adsorption data, to be described in a following section.

The inset to Fig. 1c shows that, only here and there, the $AP_{1473}a$ preparation presents also some large and irregularly shaped bulky single crystallites, of the type that is regularly met in most preparations of the α-Al_2O_3 phase (15).

Surface Chemical Data

The surface chemical behaviour of the AP_{T_1} systems has been tested by *in situ* adsorption FTIR spectroscopy, with the use of several of the test molecules normally employed in surface chemistry. For the sake of clarity, the results will be divided in sections, each dealing with a specific aspect of the alumina surface features.

The Background Spectrum

A. Surface hydroxyls. The most important and typical aspect of the background spectrum of a polydispersed oxide concerns the spectral range at $\tilde{\nu} \geq 2500$ cm^{-1},

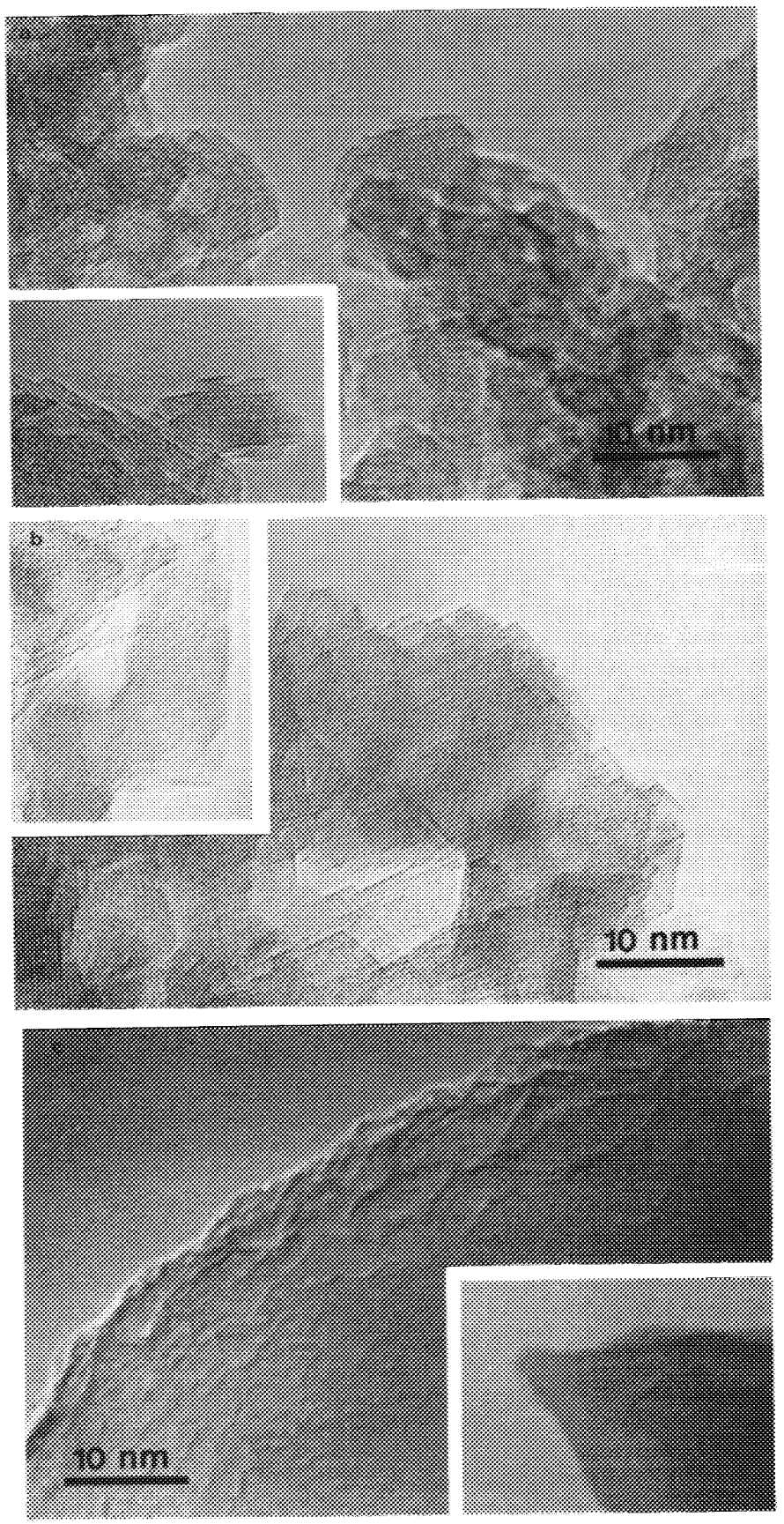

FIG. 1. TEM images of the AP_{T_1} specimens taken at high magnification. (a): AP_{773}. Inset: detail of the reference sample A_{773}; (b) and inset: AP_{1273}; (c) and inset: $AP_{1473}a$.

where absorptions are known to be due to the stretching vibrations of surface hydroxyl groups [18].

The spectral features of the ν_{OH} region of transition aluminas are quite complex, due to the double coordination of Al ions (tetrahedral (Al^{IV}) and octahedral (Al^{VI})); these features have been long investigated by several authors, and do not need here any further discussion. In particular, the description of surface OH groups and the relevant band assignment proposed for transition aluminas by Knözinger and Ratnasamy (19) is now commonly accepted, and will be here referred to without comments. The corundum phase (α-Al_2O_3) has a simpler ν_{OH} region, due to the structure involving the sole octahedral coordination of Al (Al^{VI}), and presents a couple of weak bands of variable relative intensity in the 3730–3700 cm^{-1} interval (20).

As for the effect of P-doping on the OH spectrum of transition aluminas, other authors (6, 8) have reported that the presence of phosphates leads to:

(i) A generalized decrease of the various OH species typical of transition aluminas, meaning that the anionic surface species adsorb through a sort of surface acid–base neutralization reaction, with the formation of P–O_n surface bonds. The latter can be observed in the IR spectrum in the 1200–1000 cm^{-1} region.

(ii) The appearance of a new surface OH species, absorbing at $\approx$3675 cm^{-1}, ascribed to surface P–OH groups. A strong band, centered at $\approx$3675 cm^{-1} and due to surface P–OH groups, is present also in the spectrum of various $AlPO_4$ preparations (21, 22).

Figure 2 compares the OH stretching region of few reference A_{T_1} samples and of some AP_{T_1} systems, isolated in different medium-high stages of the vacuum thermal activation (dehydration) process, and corresponding to the probable conditions of a working catalyst support.

The following can be noted.

(i) On the γ-Al_2O_3 system (curves 1–2), the presence of surface phosphates is readily documented by a weak P–OH band at $\approx$3675 cm^{-1}. The band is quite broad (due to some residual H-bondings) in the sample activated at 773 K, and becomes sharp in the sample activated at 1023 K. The spectral features of the hydroxyls due to the alumina component are very slightly modified, if at all, with respect to the pure alumina phase (compare curves 1–1* and 2–2*). In particular, the ν_{OH} band at $\approx$3775 cm^{-1} (the so called species I_a (19), ascribed to terminal OH groups on surface Al^{IV} ions), that is most readily available for reaction with all kinds of adsorbates, maintains in the presence of phosphates a virtually unchanged intensity.

The spectra of the OH region thus seem to indicate that the addition at the surface of γ-Al_2O_3 of a nominal concentration of 1.7 phosphate groups per nm^2 (i.e., slightly less than a half monolayer) leads to a mixed system, in which two different surface phases coexist.

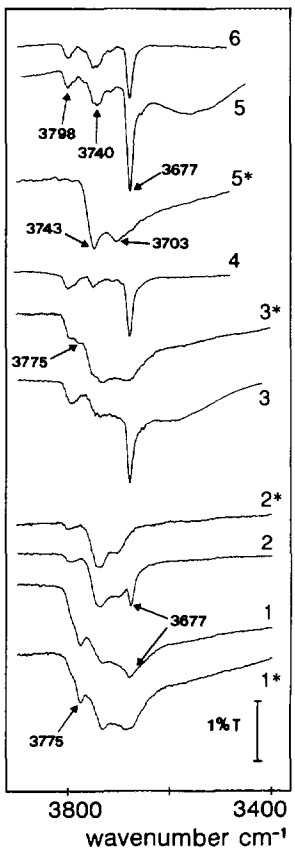

FIG. 2. Transmittance spectra, in the spectral region of the ν_{OH} modes, of some AP samples and A reference samples. Curve 1*: $A_{773}773$; 1: $AP_{773}773$; 2: $AP_{773}1023$; 2*: $A_{773}1023$; 3: $AP_{1273}773$; 3*: $A_{1273}773$; 4: $AP_{1273}1023$; 5*: $A_{1473}773$; 5: $AP_{1473}773$; 6: $AP_{1473}1023$.

(ii) On the δ, θ-Al_2O_3 system (curves 3–4), the spectrum in the ν_{OH} region is dominated by a strong, sharp P–OH peak at $\approx$3675 cm^{-1}, whereas the OH components typical of the alumina phase have been severely depleted, with the exception of the I_b component at $\approx$3800 cm^{-1} (that is known to be the far less reactive OH species at the surface of aluminas). In particular, the most active I_a OH component at $\approx$3775 cm^{-1}, that on the δ, θ-Al_2O_3 phase is usually quite weak (17) (see curve 3*), in the presence of phosphates becomes totally absent.

The OH spectral features thus indicate that, on the alumina system fired at 1273 K, the contact between the alumina and the phosphate components has become more intimate than on the γ phase, even if the nominal PO_4 content has increased only to $\approx$2.5 groups per nm^2, i.e., slightly above a value corresponding to half monolayer on the average.

(iii) On the AP_{1473} system, whose bulk after aging has become entirely α-Al_2O_3, the spectrum of the ν_{OH} region is even more severely modified with respect of the corresponding A_{1473} phase (see curves 5-6). The P-OH band

≈3675 cm^{-1} dominates the spectrum of the sample treated at 773 K, and declines much but is still dominant on the sample treated at 1023 K. There are two weak and broad Al-OH bands at ≈3800 and ≈3740 cm^{-1}, in the regions usually ascribed to mono- and bicoordinated OH groups respectively: the latter component is quite similar to the main OH component observed on A_{1473} (compare curves 5-5*), whereas the former OH band is reminiscent of the highest frequency I_a–I_b envelope of transition aluminas as well as of the terminal Al^{IV}–OH groups observed by Peri (21) on $AlPO_4$. The residual presence at the surface of AP_{1473} of some Al centers with a (quasi) tetrahedral coordination is thus inferred, and needs to be confirmed by the study of solid–gas interactions.

B. The Region of P–O Vibrations. Loading phosphates at the surface of oxides brings about the appearance of strong IR bands in the spectral region 1400–900 cm^{-1}, due to various P–O vibrations and, possibly, of P–OH deformations. In the case of alumina, the observation of these modes is limited to ≈1000 cm^{-1} if the usual self-supporting IR pellets are used, due to the strong absorption caused by Al–O skeletal vibrations.

Figure 3 reports the spectral range 1500–1000 cm^{-1} of various AP_{T_1} specimens. It is noted that all samples present a strong complex absorption, whose shape and intensity changes somewhat with thermal treatment conditions. Still, the analytical use of this spectral region is limited, as all bands of AP_{T_1} are quite similar, and the absorptions present in this region due to phosphates of different structure are not appreciably different from one another (23).

It is interesting to note that on passing from AP_{773} to AP_{1273}, when the interaction between phosphate and alumina components becomes stronger, the major spectral component of the complex P–O band moves downwards from ≈1180 to ≈1130 cm^{-1}. This indicates a decreased P–O bond order, i.e., a more pronounced character of P–O single bond, as observed in various PO_4-doped systems in which the interaction with the support is strong and the character of the various bonds involved is highly ionic (6).

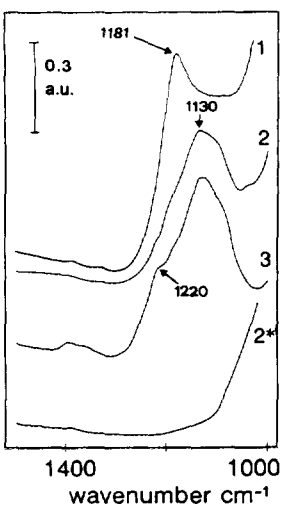

FIG. 3. Absorbance spectra in the 1500–1000 cm^{-1} range relative to PO vibrations. Curve 1: $AP_{773}1023$; 2: $AP_{1273}1023$; 3: $AP_{1473}1023$; 2*: reference $A_{1273}1023$.

Spectral P–O components at $\tilde{\nu} \geq 1200$ cm^{-1}, due to P–O bonds whose order is close to two (phosphoryl groups), are virtually absent on alumina systems treated at $T_1 \leq 1273$ K (traces 1 and 2 in Fig. 3), whereas an appreciable $\nu_{P=O}$ component is present at ≈1220 cm^{-1} in the case of AP_{1473} (trace 3 in Fig. 3). This indicates that, as long as the surface coverage of phosphates is well below a statistical monolayer, no phosphoryl-containing species of the type formed at all coverages at the surface of covalent systems (like silica (5, 6)), are produced at the surface of alumina. On the lower area α-Al_2O_3 system, on which the phosphate nominal coverage goes above a statistical monolayer, more complex phosphate structures of the polyphosphate type start forming, and some double-bonded P–O groups become observable in the IR spectrum.

Surface Basicity

Surface basicity of oxides is most often tested with the adsorption of CO_2, that yields various types of carbonate-like surface species on coordinatively unsaturated (cus) anion sites and cus anion–cation couple sites. The various carbonate-like species have characteristic spectral features (18, 24), and their assignment is relatively easy on the basis of literature data. The nature of surface carbonate-like species yields information on the nature of the surface basic centers.

The surface basicity of (spinel) transition aluminas is known to be quite low. CO_2 uptake on γ-, δ-, and θ-Al_2O_3 yields mainly two types of surface bicarbonate species (termed B_1 and B_2 (25)) in the case of aluminas dehydrated at low-to-medium temperatures, and yields increasing amounts of "organic" bridging carbonates in the case of aluminas dehydrated at medium–high temperatures. Unlike that, on non defective (corundum) α-Al_2O_3, the amount of bicarbonates and "organic" carbonates formed upon adsorbing CO_2 is negligible (26), whereas relatively abundant bidentate chelating carbonate structures are formed on cus Al^{VI}–O^{2-} couples.

Figure 4 reports the spectra of CO_2 adsorbed (under a pressure P_{CO_2} of ≈12 Torr) onto some AP_{T_1} and A_{T_1} reference samples, isolated in a medium dehydration stage. The following can be noted.

(i) On $AP_{773}773$ and $A_{773}773$, the sample-weight-normalized spectra of adsorbed CO_2 (Fig. 4a) are very simi-

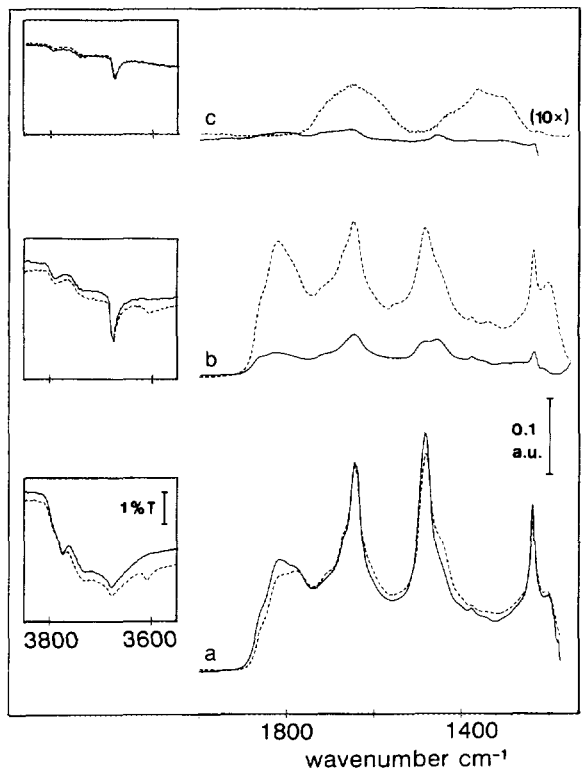

FIG. 4. Absorbance spectra in the 2000–1150 cm $^{-1}$ range, due to the formation of carbonate-like species at the surface of some AP and A reference samples upon uptake of 12 Torr CO_2. (a): $AP_{773}773$ (solid line) and $A_{773}773$ (broken line); (b): $AP_{1273}773$ (solid line) and $A_{1273}773$ (broken line); (c): $AP_{1473}a1023$ (solid line) and $A_{1473}1023$ (broken line); the spectra in (c) underwent a 10-fold Y-scale magnification. In the insets are compared the ν_{OH} regions of the three AP samples before (—) and after (- - -) CO_2 uptake.

lar, and are dominated by abundant bicarbonates of the B_2 type (bands at ≈3615, ≈1650, ≈1480, and ≈1230 cm^{-1}), very small amounts of bicarbonates of the B_1 type (the relevant $(\nu_{CO_2})_{asymm}$ mode is at ≈1440 cm^{-1}), and abundant "organic" carbonates (bands at $\tilde{\nu} \geq$ ≈1730 cm^{-1} and $\tilde{\nu} \leq$ ≈1230 cm^{-1}).

It is quite evident that, on AP_{773}, phosphates did not modify the type nor the amount of carbonate-like species formed, in the same conditions, on the pure γ-Al_2O_3 system. In particular, the inset to section 4a shows that surface bicarbonates form on $AP_{773}773$ at the expense of part of the ν_{OH} band I_a (≈3775 cm^{-1}) of alumina, as in the case of pure alumina (25), whereas all other ν_{OH} bands of alumina and the shallow ν_{OH} band due to P–OH surface groups are not involved to a detectable level in the formation of bicarbonates.

(ii) On $AP_{1273}773$ (Fig. 4b), the situation of surface carbonates formed upon CO_2 uptake has become quite different from that of the corresponding $A_{1273}773$ system. The type of carbonates formed is still the same on the two materials (there is only a modified intensity ratio between bicarbonates B_1 and B_2), but the overall intensity of the bands is much lower on the phosphate-doped system. Gas volumetric data, not reported here, confirm that CO_2 uptake is much lower on AP_{1273} than on the corresponding alumina.

The inset to Fig. 4b, relative to the ν_{OH} region, shows that also on $AP_{1273}773$ the formation of bicarbonates does not involve at all the sharp and strong P–OH band at ≈3675 cm^{-1}.

(iii) Figure 4c shows that, on the α-Al_2O_3 systems, the difference between PO_4-free and PO_4-doped systems is even stronger. $A_{1473}773$ presents broad and ill-resolved bands at 1600–1700 and 1200–1400 cm^{-1}, typical of the bidentate carbonate species formed on all α-Al_2O_3 preparations (26), whereas on $AP_{1473}a773$, in spite of the much higher surface area, virtually no carbonate-like species of any type are formed. The inset to Fig. 3c shows that, also in the ν_{OH} region largely dominated by the PO-H vibration, CO_2 uptake does not produce appreciable perturbations.

The room temperature adsorption of CO_2 so indicates that the presence of phosphates, and of P–OH groups therein, does not produce on alumina new basic centres active for CO_2 uptake. Instead, surface phosphates gradually eliminate the basic centres of alumina, and do so in a way that is not proportional to the (nominal) PO_4 surface coverage: in fact, upon activation at 773–1273 K, the PO_4 coverage changes from little less to little over half a monolayer, but the activity of alumina toward CO_2 passes from virtually unchanged to almost extinguished. The type and strength of the interaction between phosphates and the alumina network, that is a function of the firing temperature and was already brought to evidence by the background spectra of the AP_{T_1} systems, turns out to be primarily responsible for the gradual suppression of aluminas basic sites.

Surface Acidity

Several probe molecules are usually employed in IR spectroscopic experiments, in order to test the surface acidity of adsorbing systems. Among them, quite suitable are CO, CO_2 (and namely, the fraction of CO_2 that adsorbs onto surface cus cationic centres, yielding end-on complexes (27)), and pyridine (py). The information details deriving from the use of these adspecies are often complementary: for instance, the strong Lewis base py reveals (though with moderate sensitivity) virtually all families of surface acidic centres, whereas the soft Lewis base CO reveals (with great sensitivity) only the strongest fraction of surface acidic sites.

A. Carbon monoxide. In recent works (17, 28, 29) it was reported that the room temperature interaction of CO with transition-phase (spinel) Al_2O_3 systems yields

up to three adspecies termed, in order of increasing ν_{CO} stretching frequency, $(CO)_A$, $(CO)_B$, and $(CO)_C$ respectively. The former species, that is by far the most abundant one, has been demonstrated [27, 29] to correspond to CO uptake onto cus Al^{IV} sites located on flat patches of regular low-index crystal planes, whereas the other two species correspond to the adsorption onto cus Al^{IV} ions located in two families of crystallographically defective configurations. These configurations are thought to be mainly responsible for the high acidity of transition phase aluminas.

Unlike that, on the corundum phase α-Al_2O_3, no CO uptake can be observed at ambient temperature (20), due to the very low Lewis acidity of cus Al^{VI} ions.

Figure 5 reports IR spectral patterns relative to the adsorption at ≈300 K of CO onto some AP_{T_1} systems. The following can be noted.

(i) On the γ-Al_2O_3 system (Figs. 5a and 5b) the spectra of adsorbed CO exhibit overall intensities comparable with those of the corresponding pure alumina (see the broken line traces in 5a and 5b), but the relative intensity and spectral position of the various CO adspecies tend to be altered. In particular, the sample treated at lower temperature ($AP_{773}773$, 5a) exhibits only a slightly increased intensity of the $(CO)_C$ species (≈2236 cm^{-1}) and $(CO)_B$ species (≈2215 cm^{-1}), whereas the sample treated at higher temperature ($AP_{773}1023$, Fig. 5b; note that the sample was activated at a temperature higher than that of the first firing treatment, a situation frequently met in catalytic applications) exhibits a slightly increased band $(CO)_C$ and a band $(CO)_B$ appreciably increased. In the latter sample, the relative intensity of the species $(CO)_A$, due to CO adsorbed on sites on regular crystal faces, is lower than on pure alumina, and in both $AP_{773}T_2$ samples the band of the $(CO)_A$ species tends to lie at slightly higher wavenumbers than on pure alumina.

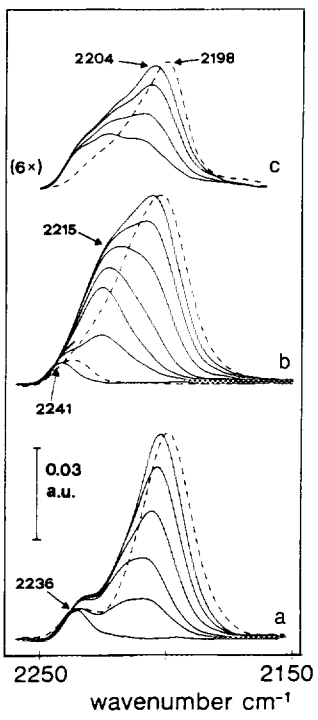

FIG. 5. IR spectral patterns relative to the adsorption at ≈300 K of CO onto some AP and A reference systems (p_{CO} varied from 10^{-1} to 90 Torr). (a): $AP_{773}773$; broken line: 90 Torr CO onto $A_{773}773$. (b): $AP_{773}1023$; broken lines: 90 and 10^{-1} Torr CO onto $A_{773}1023$. (c): $AP_{1273}1023$; broken line: 90 Torr CO onto $A_{1273}1023$. The spectra in (c) underwent a six-fold Y-scale magnification.

(ii) On the δ, θ-Al_2O_3 system (Fig. 5c), the effects already observed for the γ phase are dramatically enhanced. In fact, the $AP_{1273}1023$ sample presents abundant $(CO)_C$ and $(CO)_B$ "defective" components (that are quite scarce on the corresponding pure alumina, as shown by the broken-line trace), whereas the "regular" $(CO)_A$ species is much less abundant than on alumina, and is shifted upwards by ≈6 cm^{-1}.

Note that, on the $AP_{1473}a$ α-Al_2O_3 system, no CO uptake is observed at 300 K after thermal activation at any T_2 temperature.

The present data relative to CO adsorption tend to give a more detailed meaning to the slight increase of acidity observed by some authors, and induced in the transition alumina phases by the presence of phosphates. In fact, it can be deduced that:

(i) As long as the alumina is in the γ phase and, more important, the solid has been treated at relatively low temperatures ($T \leq$ ≈600 K), the interaction between phosphates and the alumina network is modest, as also suggested by the OH patterns, and two virtually separated oxidic systems exist at the surface of the AP preparation. The strong Lewis acidity of alumina is almost unchanged, much as unchanged is the basicity of the alumina support.

(ii) When the alumina is treated at higher temperatures ($600 \leq T \leq 1300$ K; the phase either remains γ or becomes δ–θ), the interaction with phosphates becomes stronger. A real acid–base surface reaction starts occurring, and affects both chemical and structural features of the AP preparation. The population of Lewis acid sites located on regular crystal faces declines, suggesting that the regular crystal faces of alumina are the favoured site for PO_4 adsorption, whereas the population of stronger Lewis acid sites located in crystallographically defective configurations increases appreciably. Moreover, the spectral position of all CO adspecies tends to increase, due to inductive effects from the surface phosphate groups that induce a stronger charge release from adsorbed CO to the cus Al^{IV} adsorbing sites. This effect is well-known in the case of ionic oxides carrying surface

anions, like carbonates (30) and sulfates (31), but was not reported so far for surface phosphates.

(iii) When the alumina is treated at $T \geq \approx 1450$ K (and aged for long time), so that the α phase is produced, all the strong Lewis acid centres capable of chemisorbing CO at ambient temperature are suppressed. This can occur either because at the surface remain only inactive cus (Al^{VI}) centers (as expected of a regular corundum phase), or because the whole surface is covered by thermally stable phosphate groups and no cus Al ions remain accessible. To check this point, the use of other probe molecules will thus be resorted to.

B. End-on carbon dioxide. The observation of the Σ_u^+ mode of linearly coordinated CO_2 is a useful tool in surface chemistry, as this probe molecule possesses high extinction coefficient (and thus high spectroscopic sensitivity) and can reveal various families of surface Lewis acid sites of different strength (27). In the case of alumina, end-on adsorbed CO_2 yields bands at ≈ 2345 cm^{-1} that are ascribable to very weak Lewis sites (like, for instance, cus Al^{VI} centers, not revealed by CO), and bands at $\tilde{\nu} \geq 2350$ cm^{-1}, ascribable to stronger Lewis sites whose strength is higher the higher the spectral position of the relevant Σ_u^+ mode (15).

Figure 6 reports some spectra of CO_2 linearly held at the surface of AP_{T_1} systems, compared with the corresponding pure alumina. It can be noted that:

(i) In the material fired and activated at the lowest temperatures considered here, the spectral features of CO_2 adsorbed on AP and A samples are very similar, though not identical (see Fig. 6a). In particular, the sharp peak due to CO_2 onto cus Al^{VI} centers (≈ 2345 cm^{-1}) dominates on both systems, and the broad absorption at ≈ 2365 cm^{-1} (cus Al^{IV} centers) is slightly stronger on the AP sample.

(ii) In the δ, θ-Al_2O_3 AP_{1273} system (see Fig. 6b), in which the interaction of the phosphates with the alumina network has become stronger, the end-on CO_2 component(s) absorbing at $\tilde{\nu} \geq 2360$ cm^{-1} have become much stronger than on A_{1273}. This confirms the indication given by CO uptake: on transition-phase AP aluminas, the presence of phosphates delays the annealing of the most defective structural configurations that carry the most energetic cus Al^{IV} sites, so that the overall acidity of the systems turns out to be stronger than that of the corresponding pure alumina systems.

(iii) In the $AP_{1473}a773$ system (see the lower-lying curves in Fig. 6c), in which the bulk phase transformation to α-Al_2O_3 has occurred thoroughly, the overall absorption due to linearly held CO_2 is definitely much stronger than on A_{1473}, as a consequence of the higher surface area. Moreover, the band of end-on CO_2 surface complexes still presents an appreciable component at $\tilde{\nu} \geq 2350$ cm^{-1}, broad and heterogeneous, whereas the corresponding A_{1473} system has only the sharp peak at ≈ 2345 cm^{-1} due to cus Al^{VI} sites. This indicates that the aging process and the slow phase transformation ($\delta, \theta \rightarrow \alpha$) has left at the surface of the crystallites a relatively high amount of crystallographic and/or coordinative defective situations, in which Al ions with a (quasi-)tetrahedral coordination are present. The latter surface centres result to be Lewis acidic sites not strong enough to chemisorb CO at ambient temperature, but still capable of coordinating CO_2 with $\tilde{\nu} \geq 2350$ cm^{-1}.

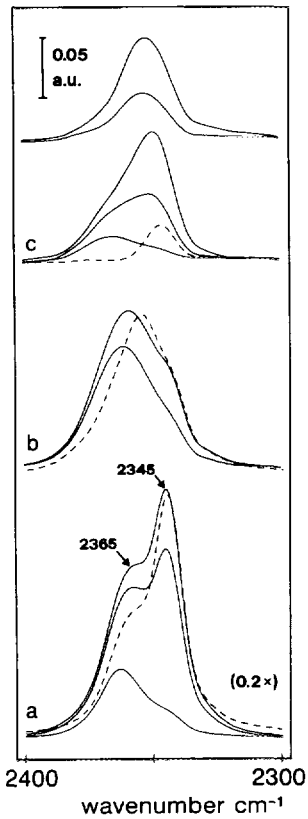

FIG. 6. Absorbance spectra, in the spectral range of the Σ_u^+ mode of CO_2, due to the formation of end-on CO_2 complexes onto some AP (solid lines) and A reference samples (broken lines). P_{CO_2} was decreased from 12 Torr to 5 Torr (when two curves are reported) and then to 0.1 Torr (when three curves are reported). (a): $AP_{773}773$; the broken-line trace corresponds to the uptake of 12 Torr CO_2 onto $A_{773}773$. These spectra underwent a 0.2-fold ordinate scale reduction. (b): $AP_{1273}1023$; the broken-line trace corresponds to the uptake of 12 Torr CO_2 onto $A_{1273}1023$. (c), lower curves: $AP_{1473}a773$; the broken line trace corresponds to the uptake of 12 Torr CO_2 onto $A_{1473}773$; (c), upper curves: $AP_{1473}a1023$.

The upper curves of Fig. 6c indicate that, on increasing the temperature of vacuum activation of the $AP_{1473}a$ system, the intensity of the end-on CO_2 components at $\tilde{\nu} \geq 2350$ cm^{-1} declines. This is most surprising and suggests that the system is still metastable and can undergo further changes: either the process of crystallization and conse-

quent loss of surface area is still occurring and can be accelerated by the high temperature treatment in vacuo, or the long exposure of the material to the atmosphere hydrolyzed part of the Al–O–P bondings, with formation of some P–OH and Al–OH groups. The latter can dehydrate at medium activation temperatures, yielding cus Al^{3+} sites capable of adsorbing CO_2, and at higher activation temperatures can reproduce the Al–O–P linkages, thus reducing the activity towards CO_2 uptake. Experiments of CO_2 adsorption after rehydration/second dehydration of A_{1473}a samples (not described in detail) indicate that the second hypothesis is more realistic.

C. Pyridine. After the first pioneering work by Parry (32), py has been widely used to test the surface acidity of oxidic systems. In particular, the system py/Al_2O_3 has been studied by several authors and has been reviewed recently (14, 33).

Figure 7 reports, for some AP_{T_1} and reference A_{T_1} specimens, the analytical IR spectral region of py adsorbed at ambient temperature (under a moderate py pressure) and evacuated at ambient temperature. The following can be noted.

(i) In none of our AP materials, in spite of the presence of P–OH groups, changes of crystal phase, and changes of phosphate coverage (that ranges from approximately half a monolayer to over a nominal monolayer), could we ever observe any evidence for the formation of $[py\text{-}H]^+$ species, whereas $[py\text{-}H^+]$ species were observed in the case of other PO_4-doped aluminas (5, 7, 9). In particular, the Brønsted acidity is absent also in the case of highly hydrated AP samples (see, for instance, the case of $AP_{773}300$ in Fig. 7a; the vertical arrow indicates the position where $[py\text{-}H]^+$ would absorb, if present); in these materials there is a very strong interaction of py with surface OH groups, but through a mere perturbation of the H-bonding type, as monitored by the strong 8a py mode at $\approx 1590\ cm^{-1}$.

These observations indicate that surface phosphates,

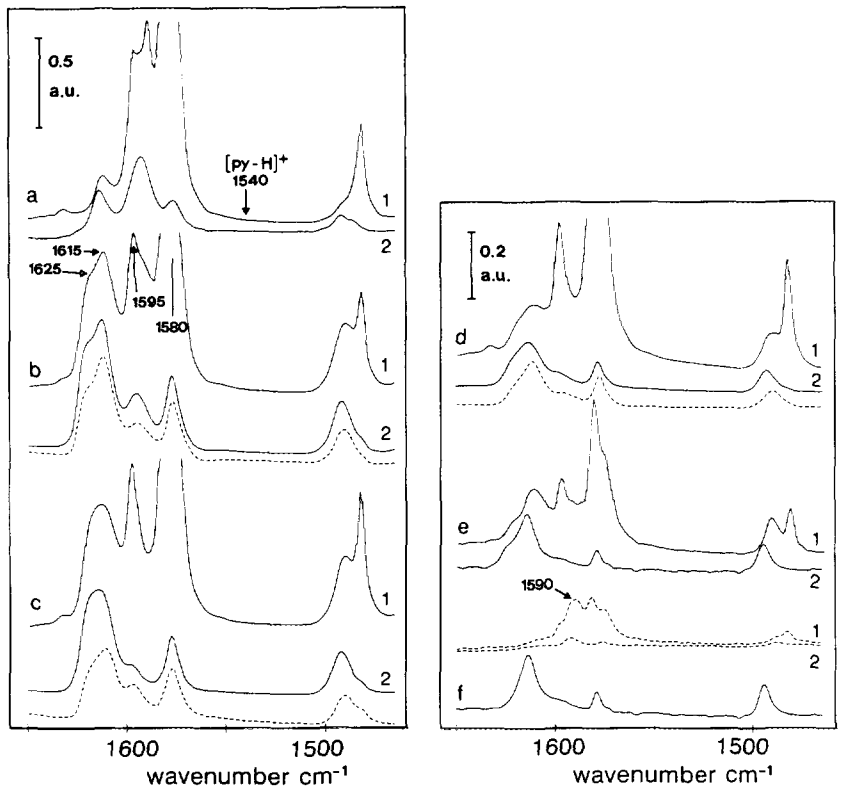

FIG. 7. Absorbance spectra in the 1650–1465 cm^{-1} range obtained after adsorption of py onto some AP and A reference samples and subsequent py evacuation at ambient temperature. (a): 8 Torr pyridine adsorbed onto $AP_{773}300$ (curve 1) and evacuated for 5 min at ambient temperature (curve 2); the arrow indicates the position where $[py\text{-}H]^+$ would absorb, if present. (b): 8 Torr pyridine adsorbed onto $AP_{773}773$ (curve 1) and evacuated at ambient temperature (curve 2); broken-line curve: $A_{773}773$, py adsorbed and evacuated for 5 min at ambient temperature. (c): 8 Torr pyridine adsorbed onto $AP_{773}1023$ (curve 1) and evacuated at ambient temperature (curve 2); broken-line curve: $A_{773}1023$, py adsorbed and evacuated at ambient temperature. (d): 8 Torr pyridine adsorbed onto $AP_{1273}773$ (curve 1) and evacuated at ambient temperature (curve 2); broken-line curve: $A_{1273}773$, py adsorbed and evacuated at ambient temperature. (e): 8 Torr pyridine adsorbed onto $AP_{1473}773$ (curve 1) and evacuated at ambient temperature (curve 2); broken-line curves: 8 Torr pyridine adsorbed onto $A_{1473}773$ (curve 1) and evacuated at ambient temperature (curve 2). (f): pyridine adsorbed and evacuated at ambient temperature onto $AP_{1473}1023$.

and P-OH groups thereon, are not capable per se of forming pyridinium species. Other aluminas or, more likely, other (i.e., higher) PO_4 coverages are needed to yield, also at the surface of alumina, that sort of "supported phosphoric acid" phase that can form pyridinium ions, like in the case of PO_4-doped silica (5).

(ii) The spectral patterns of Figs. 7a and 7b show that, on the γ-phase AP_{773} samples activated at $T_2 \geq 773$ K, the interaction with py yields different amounts of three families of Lewis coordinated adspecies, whose 8a modes lie at $\approx$1625, $\approx$1615, and $\approx$1595 cm^{-1} respectively. The three species have been previously ascribed to py adsorbed onto coordinative vacancies located on Al^{IV}, Al^{IV}-Al^{VI} pairs, and Al^{VI} sites respectively (34). The broken-line spectra in Figs. 7b and 7c indicate that also py adsorption cannot reveal appreciable differences between AP_{773} and A_{773} samples.

(iii) Figure 7d shows that, on the δ, θ-phase AP_{1273} samples, there is a decline of the relative intensity of the strongest py adspecies (8a mode at $\approx$1625 cm^{-1}), ascribed to the strongest family of Lewis acid sites. This decline is expected, on the basis of the behavior exhibited by the strongest Lewis acid sites of alumina further to $\gamma \rightarrow \delta, \theta$ phase transition (17), but is less abundant than in the case of the corresponding pure alumina system (see the broken-line spectrum in Fig. 7d). This result is consistent with the information given by the adsorption of CO and end-on CO_2: in fact, all CO adspecies formed on alumina at ambient temperature and all linear CO_2 adspecies absorbing at $\tilde{\nu} \geq 2350$ cm^{-1} correspond to the sole py adspecies whose 8a mode is at $\approx$1625 cm^{-1}, whereas the other py adspecies correspond to cus cationic sites too weak to coordinate CO at ambient temperature or to coordinate CO_2 with $\tilde{\nu} \geq 2350$ cm^{-1}.

(iv) On the AP_{1473} system, the adsorption of py reveals the strongest differences with respect to pure alumina. In fact Fig. 7e shows that the spectral pattern of py uptake onto $AP_{1473}a773$ is still that typical of a transition phase alumina, with three families of py species coordinated to Lewis acid sites, two of which involve surface cus Al^{IV} sites. Opposite to that, the spectrum of py on the real α-Al_2O_3 system $A_{1473}773$ (see the broken-line traces in Fig. 7e) is much weaker, due to the much lower surface area, and presents 8a and 8b bands at lower frequencies ($\approx$1590 and $\approx$1575 cm^{-1}), typical of the purely octahedral coordination of Al ions in the corundum phase. This indicates that, despite the complete bulk phase transformation to α-Al_2O_3 achieved by the AP_{1473} system, a still relatively high surface area is accompanied by surface termination configurations in which the tetrahedral or quasi-tetrahedral occupation of Al ions is still abundant.

The last trace in Fig. 7f, relative to py uptake onto $AP_{1473}a1023$, shows that on the system activated at higher temperature the py band at $\approx$1625 cm^{-1}, due to the strongest cus Al^{IV} sites, has declined. This confirms the indication already given by the end-on adsorption of CO_2: the surface of the α-phase $AP_{1473}a$ system is unstable, and activation at high temperatures reduces the number of strong acid sites exposed (a plain dehydration would increase it), most likely as a consequence of a stronger surface interaction between the alumina and the phosphate components.

CONCLUSIONS

The data presented in this note explain: (i) What is the actual role played by the addition of moderate amounts of phosphates to alumina. This addition is frequently done in the case of aluminas used as active catalytic supports. (ii) What is the actual meaning of the phase stabilization effect produced by the addition of phosphates. This effect is often claimed in the case of PO_4-doped aluminas employed as catalyst supports.

A. As far as the bulk features of Al_2O_3 are concerned, the addition of phosphates does not modify the phase transition of low-temperature spinel aluminas to high-temperature spinel aluminas (1), and delays somewhat the phase transition from spinel alumina to corundum.

B. As for the morphology of the alumina particles, further to phosphates addition it turns out to be: slightly modified with respect to that of pure alumina in the γ-phase, when the surface chemical properties are virtually unchanged, to be almost unchanged in the δ, θ-phase, when the surface chemical properties are abundantly modified, and to be appreciably modified in the α-phase, when the changes of surface chemical properties are at a maximum.

C. As for the other significant macroscopic physical properties of aluminas, namely the high surface area and porosity, the addition of phosphates is expected to have a positive effect. This work shows that this is partly true only for the corundum phase, obtained at $T_1 \geq 1450$ K, (in which also the particles morphology is modified with respect to the pure α-Al_2O_3 phase). Unlike that, in the transition phases stable at $T_1 < \approx 1400$ K, the surface area is appreciably decreased by the presence of phosphates.

D. When the detailed chemical properties of the AP materials are considered, the effect of adding to alumina moderate amounts of phosphates turns out to be appreciable and twofold.

(i) The type of (weak) surface basic sites presented by alumina is, in general terms, unchanged, but the amount of these basic sites is gradually diminished and replaced by the thermally stable phosphates. The extent to which the surface basicity of aluminas is suppressed depends on the firing temperature rather than on the surface coverage of phosphates. In fact the interaction of phosphates with the alumina network becomes stronger

the higher the firing temperature of the PO_4-doped system, whereas the surface area of the system declines more slowly.

(ii) The surface acidity of the alumina is gradually modified (and in general terms increased) by the stronger and stronger interaction between phosphates and the alumina support achieved at increasing firing temperatures. Phosphates tend to collect preferably on the flat patches of regular crystal planes of the alumina system, and so doing decrease the amount and increase the strength of the Lewis acid sites (cus Al^{IV} ions) present on the regular crystal planes. Meanwhile, the presence of phosphates, that induces a moderate change of the morphology of crystallites, produces an appreciable increase of the number (and possibly of the strength) of cus Al^{IV} Lewis acid sites present in crystallographically and/or coordinatively defective configurations.

The latter effect is particularly evident in the case of the alumina systems treated at high temperatures ($T_1 \geq 1400$ K), for which the bulk transition to the undesired α-Al_2O_3 phase has already occurred, but in which the surface acid chemical behavior is still largely that of the transition alumina phases.

As Lewis acid centers of the highest acidity are active sites for which the catalytic properties of alumina are appreciated, the diffuse opinion that phosphates act as phase stabilizing agents towards alumina should be modified. In fact, the role of phosphates should be considered in the sense that surface phosphates induce, in the various (regular) phases of alumina obtained at $T_1 \geq \approx 1000$ K, the presence of higher amounts of the strong Lewis acid sites that are most likely important in catalytic applications.

ACKNOWLEDGMENT

This work was partly financed with funds from the CNR (Rome), Progetto Finalizzato Materiali Speciali.

REFERENCES

1. Lippens, B. C., and Steggerda, J. J., *in* "Physical and Chemical Aspects of Adsorbents and Catalysts" (B. G. Linsen, M. H. Fortuin, C. Okkersee, and J. J. Steggerda, Eds.), p. 171, Academic Press, London, 1970.
2. Gishti, K, Iannibello, A., Marengo, S., Morelli, G., and Tittarelli, P., *Appl. Catal.* **12,** 381 (1984).
3. Berteau, P., and Delmon, B., *Catal. Today* **5,** 121 (1989).
4. Berteau, P., Kellens, M. A., and Delmon, B., *J. Chem. Soc. Faraday Trans.* **87,** 1425 (1991).
5. Ramis, G., Busca, G., Lorenzelli, V., Rossi, P. F., Bensitel, M., Saur, O., and Lavalley, J. C., "Proceedings, 9th International Congress on Catalysis, Calgary, 1988" (M. J. Phillips and M. Ternan, Eds.), p. 1874. Chem. Institute of Canada, Ottawa, 1988.
6. Busca, G., Ramis, G., Lorenzelli, V., Rossi, P. F., La Ginestra, A., and Patrono, P., *Langmuir* **5,** 911 (1989).
7. Ramis, G., Rossi, P. F., Busca, G., Lorenzelli, V., La Ginestra, A., and Patrono, P., *Langmuir* **5,** 917 (1989).
8. Lewis, J. M., and Kydd, R. A., *J. Catal.* **132,** 465 (1991).
9. Abbatista, F., Delmastro, A., Gozzelino, G., Mazza, D., Vallino, M., Busca, G., and Lorenzelli, V., *J. Chem. Soc. Faraday Trans.* **86,** 3653 (1990).
10. Arata, K., *Adv. Catal.* **37,** 165 (1990).
11. Norman, C. J., Goulding, P. A., and Moles, P. J., *in* "Acid–Base Catalysis II" (Sapporo (Japan), 2–4. 12. 1993), Stud. Surf. Sci. Catal., Vol. 90 (H. Hattori, M. Misono, and Y. Yono Eds.), p. 269. Elsevier, 1994.
12. Mennour, A., Ecolivet, C., Cornet, D., Hemidy, J. F., Lavalley, J. C., Mariette, L., and Engelhard, P., *Mater. Chem. Phys.* **19,** 301 (1988).
13. Patent TO91A0601, deposited by Centro Ricerche Fiat and Fiat Auto, Turin (Italy).
14. Morterra, C., Magnacca, G., Fillippi, F., and Giachello, A., *J. Catal.* **137,** 346 (1992).
15. Morterra, C., Magnacca, G., Cerrato, G., Del Favero, N., Filippi, F., and Folonari, C. V., *J. Chem. Soc. Faraday Trans.* **89,** 135 (1993).
16. Baraton, M. I., and Quintard, P., *J. Mol. Struct.* **79,** 337 (1982).
17. Morterra, C., Bolis, V., and Magnacca, G., *Langmuir* **10,** 1812 (1994).
18. Little, L. H., *in* "Infrared Spectra of Adsorbed Species," Chap. X, p. 228. Academic Press, London, 1966.
19. Knözinger, H., and Ratnasamy, P., *Catal. Rev. Sci. Eng.* **17,** 31 (1978).
20. Morterra, C., Magnacca, G., and Del Favero, N., *Langmuir* **9,** 642 (1993).
21. Peri, J. B., *Discuss. Faraday Soc.* **52,** 55 (1971).
22. Rebenstorf, B., Lindblad, T., and Andersson, L. T., *J. Catal.* **128,** 293 (1991).
23. Bellamy, L. J., *in* "The Infra-red Spectra of Complex Molecules" p. 347. Chapman and Hall, London, 1975.
24. Busca, G., and Lorenzelli, V., *Mater. Chem.* **7,** 89 (1982).
25. Morterra, C., Zecchina, A., Coluccia, S., and Chiorino, A., *J. Chem. Soc. Faraday Trans. I* **73,** 1544 (1977).
26. Morterra, C., Coluccia, S., Ghiotti, G., and Zecchina, A., *Phys. Chem. N. F.* **104,** 275 (1977).
27. Morterra, C. Cerrato, G., and Emanuel, C., *Mater. Chem. Phys.* **29,** 447 (1991).
28. Ballinger, T. H., and Yates, J. T., Jr., *Langmuir* **7,** 3041 (1991).
29. Marchese, L., Bordiga, S., Coluccia, S., Martra, G., and Zecchina, A., *J. Chem. Soc. Faraday Trans.* **89,** 3483 (1993).
30. Morterra, C., Orio, L., and Emanuel, C., *J. Chem. Soc. Faraday Trans.* **86,** 3003 (1990).
31. (a) Bensitel, M., Saur, O., Lavalley, J. C., and Mabilon, G., *Mater. Chem. Phys.* **17,** 249 (1987). (b) Morterra, C., Bolis, V., Cerrato, G., and Magnacca, G., *Surf. Sci.* **307–309,** 1206 (1994).
32. Parry, E. P., *J. Catal.* **2,** 371 (1963).
33. Zecchina, A., Coluccia, S., and Morterra, C., *Appl. Spectrosc. Rev.* **21,** 259 (1985).
34. Morterra, C., Chiorino, A., Ghiotti, G., and Garrone, E., *J. Chem. Soc. Faraday Trans. I* **75,** 271 (1979).